

CHAPTER 6: RESULTS

6.1. INTRODUCTION

The sEMG information from 8 different patients are recorded and discussed in this section. The the Simulink® implementation demonstrates the functionality of the sEMG platform. The accuracy of the sensor decoding algorithm will not be tested. The sensor decoding algorithm uses a PDM servo motor. The motor is visual output indicating whether the individual want to close or open his/her hand. The visual feedback on a person's gestures should not be underestimated, and is also demonstrated in this chapter.

The testing of the hardware includes the frequency response, the effectiveness of the calibration algorithm, and the signal to noise ratio comparison of the two hardware versions to demonstrate the effectiveness of a well planned PCB layout.

Before results are given, research results from related research in the past are revised to obtain knowledge in which biometric and biomimetic data is regarded as important results. Biometric and biomimetic data describe human characteristics and biomechatronic device performance respectively. The results chapter concludes with the testing of the sEMG platform in two special cases.

6.2. BIOMETRIC DATA

Biometric studies are the science and technology of the collecting, measuring and statistically analysing biological data. Biometric studies have a list of important parameters to describe any human function or feature [21]. Repeatability is an issue addressed in this project, and the biometric data collected, focuses on uniqueness in data for different patients.

Previous studies have focused on electrode function for different amount of hair on patients' skin [49]. Although it is clear that hair has a great effect on the electrodes' performance, there exist numerous hair-removal techniques if the sEMG platform does not work on patients with large amount of hair on the forearms.

Body types of patients and fat-percentages underneath the skin are more difficult to manage than the removal of hair. Some patients find it difficult to lose weight, and it takes time for patients to lose weight. Women have by default larger fat-percentages underneath their skin than men. The body type of each patient is regarded as important biometric data for this study. The classification of patient body types is the skinny ectomorphs, the endomorphs who have full figures, and the in-between mesomorphs. Figure 72 illustrates the three body types.

6.3. BIOMIMETIC DATA (BIOMIMICRY)

This sEMG platform will be used in an artificial hand design to mimic a natural hand. The biomimetic data captured in the simulation includes the position plot as well as the force plot compared to the reference position given through visual feedback using the animation in Simulink®. Figure 73 is an illustration of a personal sEMG recording done with the Simulink® decoding implementation.

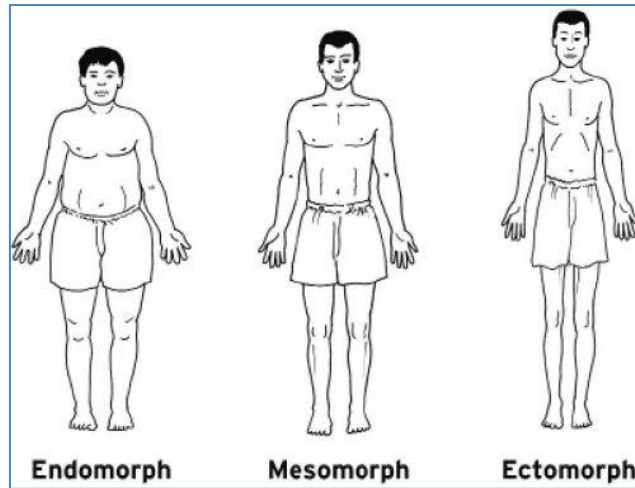


Figure 72: The three body types

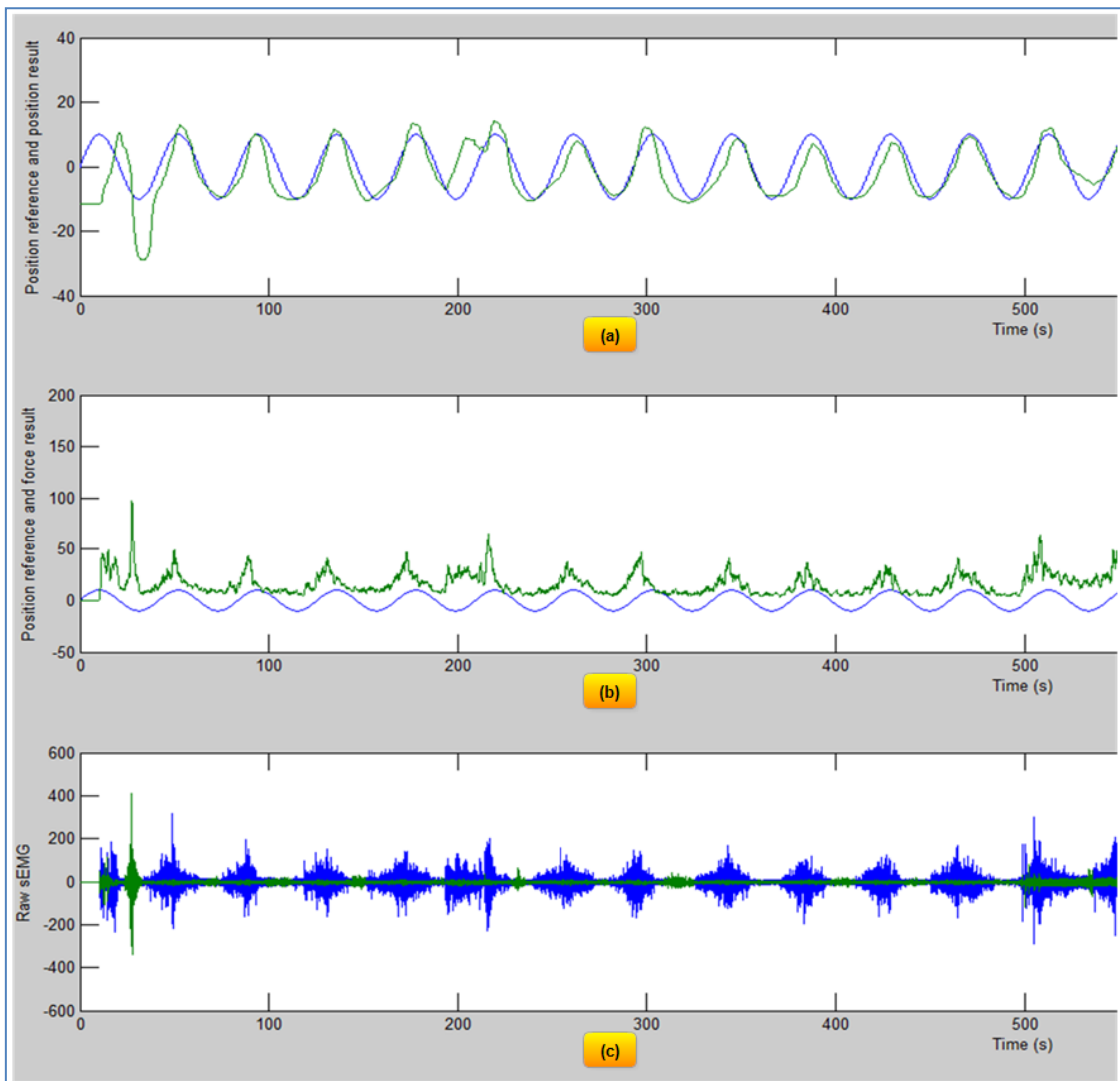


Figure 73: sEMG recording example

All sEMG information that follows throughout this chapter is presented in the format discussed in this paragraph. Figure 73 (a) shows the reference position as a blue sine wave. This is the reference given to the animation to animate an oscillating gesture. The mimicking of the opening and closing of a

hand is done by the output of the animation. The animation follows the sine waveform. The green graph is the position result decoded by the decoding algorithm. Figure 73 (b) is the reference position (blue sine wave) plotted with the proportional control algorithm's force result (green graph). Figure 73 (c) are the raw sEMG signals captured from the antagonist extensor and flexor muscles of the hand located in the forearm.

6.4. PERFORMANCE MEASUREMENT

Two different measures can either be considered to give a performance measurement of the sensing algorithm. These measure are accuracy and precision. The difference between accuracy and precision is illustrated in figure 74.

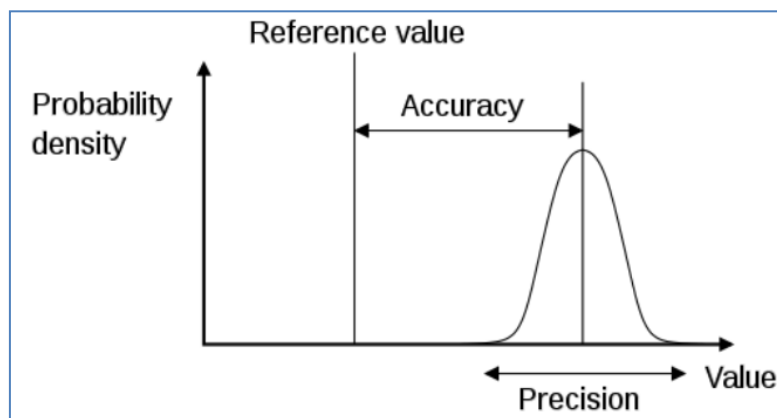


Figure 74: Accuracy and precision [50]

Accuracy is the parameter used to describe the distance the mean result deviates from the target value, or reference value. This translates to the measure describing a dc-offset in the results for this project. Precision is the parameter describing the spread of the data. Repeatability of results in this project is measured by the precision of the results.

6.5. BIOMIMETIC RESULTS OF THE PROPORTIONAL CONTROL MODEL

The graphical user interface (GUI) in Simulink[®] displays an animation, and captures the patient's sEMG data before it decodes it into position and force information. The data captured for a single patient can be viewed in figure 75. Two experiments are performed with each patient's sEMG recording process. The two sets of data captured are used to demonstrate the effect of (and importance of) visual feedback.

The two datasets are displayed in the format illustrated by figure 75. The graphs in the left column are results obtained from a patient who did not have visual feedback when the sEMG recording was made. The description of each graph is explained in section 6.3. The graphs in the right column are results obtained from the same patient with a significant improvement in results in the second experiment performed with visual feedback.

Although the precision of the result graph from the position plots is similar in both simulations (graph shape of results are similar in amplitude and shape), the accuracy of the result increases when the patient has visual feedback and intuitively corrects the offset in the system. Although the force result has not been tested for accuracy, it serves as a measure of total muscle effort of both flexor and extensor muscle groups.

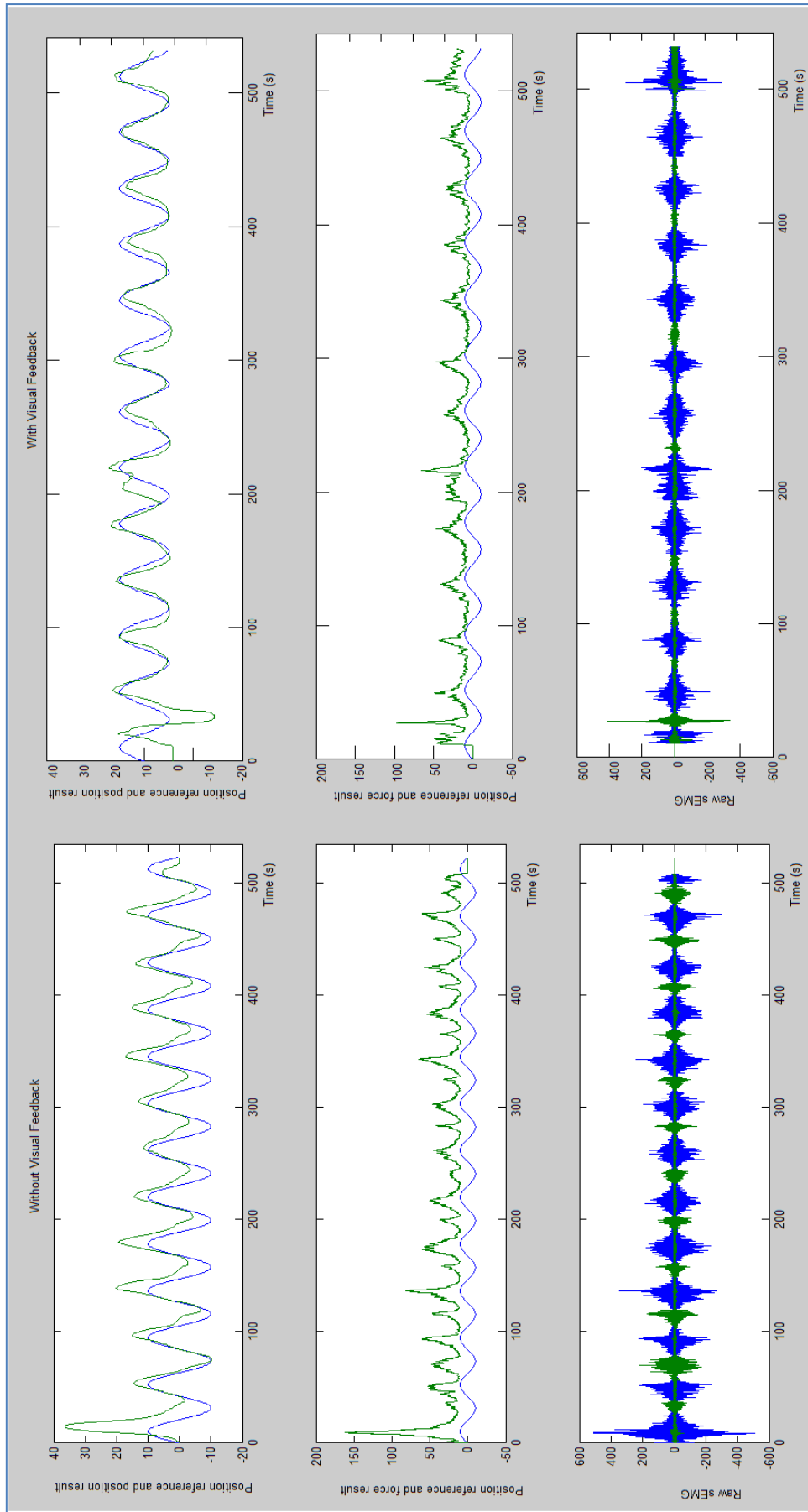


Figure 75: Results with and without visual feedback

6.5.1. INDIVIDUAL RESULTS

The correlation coefficient is calculated by calculating the average distance between each of the decoded positions from their corresponding reference position as a percentage from the maximum reference amplitude [50]. The formula for the correlation coefficient, r , is

$$r = \frac{\sum_{n=1}^{length(reference())} (1 - \frac{|L|}{max(reference())})}{length(reference())}, \quad 6-1$$

$$L = reference(n) - r(n), \quad 6-2$$

where $length()$ is a function used to determine the length of the array, $max()$ is the function used to determine the maximum value of any element contained by the array, and L is the distance between individual result and the reference values.

The results of all the patients who performed the experiment are given in table 4. The correlation shows the relationship between the position reference and the actual measurement [50].

Table 5: Simulation Results

Patient ID	Gender	Age (Years)	Body Type	Sensitivity Gain	Position Results (correlation coefficient)	
					No Visual Feedback	With Visual Feedback
1	Female	13	Mesomorph	2	0.4047	0.4548
2	Female	17	Mesomorph	1.5	0.2372	0.7823
3	Male	49	Endomorph	6	-1.1279	0.5305
4	Female	41	Endomorph	8	0.3276	0.5074
5	Female	20	Mesomorph	5	0.4104	0.6132
6	Male	25	Mesomorph	1	0.6942	0.7347
7	Male	55	Mesomorph	1.5	-5.0052	0.3003
8	Male	27	Ectomorph	0.5	0.4547	0.7327

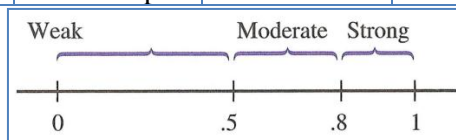


Figure 76: Interpretation of correlation coefficient [50]

The range of values for r is described by $-\infty < r \leq 1$, and the interpretation of the correlation coefficient, r , is illustrated in figure 76. The value of $r = 1$ means that the position is a perfect position follow of the animation (no human error and no sEMG error), and any value below zero means the error of the sEMG position result is greater than the animation's reference position.

The sensitivity gain is a slider gain functional block used in Simulink[®] to adjust the output of the decoding algorithm. This gain is based purely on personal preference. Each person's gain value is given in the table 4.

6.5.2. MOST PRECISE RESULTS

The most precise result is from a personal sEMG recording (patient number five). There is a noticeable improvement in a series of simulation results over a few months, suggesting that the adaption to the technology could be promising. The best and worst results could be compared by comparing the position graphs from figure 77 the graphs shown in figure 79.

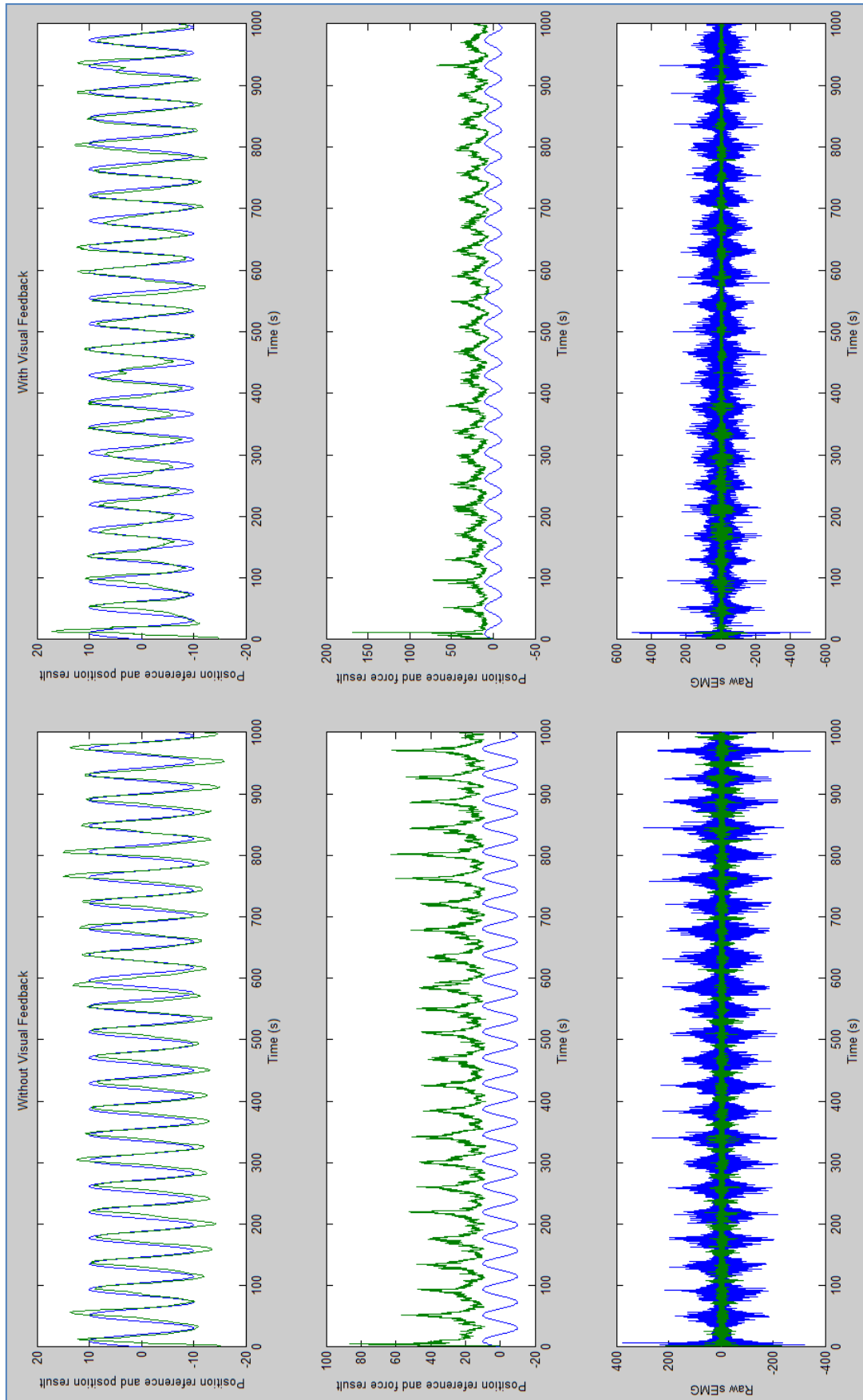


Figure 77: Best mimic results

6.5.3. WORST RESULTS

Patient seven showed the worst results. There is a tendency amongst the patients that suggests that age plays a role in the adaption of the idea that one should follow a gesture with the PDM servo rather than their normal hand. The problem is due to sudden DC-offset steps in the information. This can be viewed in figure 79. These sudden steps in the data are movement artefacts caused by the bending of the wrist.

6.5.4. AVERAGE RESULTS

An average percentage position offset of 58.2% is achieved with visual feedback, when patients follow the animation's position with the PDM servo output as reference. This average result accuracy percentage according to statistic results is not a strong correlation, but a personal rating of the average result would be, that it is relative to what is considered perfect. Consider a scenario where a normal person is asked to draw a freehand sketch of a sine function on paper, and compare it to a perfect drawing. It is already known that there would always be imperfection in gestures amongst humans. This means that the accuracy of the proportional control algorithm is the combined accuracy of the proportional control model and the patient's accuracy of following the animation's position. An average percentage offset of 140% is achieved without visual feedback, showing the effect visual feedback has on the patient's accuracy following the animation's position.

6.6. CIRCUIT PERFORMANCE

This section describes the technical results of the design, which includes the frequency response, the SNR, and the calibration of the sensors.

6.6.1. EXPERIMENTAL RESULTS

The prototyping platform suggests that the required total gain value for the final design of the sEMG amplifier should be around 500 to utilise the full range of the microcontroller's ADC. The prototyping platform resulted in only one PCB layout version required. This lowered the cost of the design process.

6.6.2. FREQUENCY RESPONSE

Experimental sEMG signals shows large energy density between 100Hz to 450Hz. Figure 78 illustrates the frequency spectrum of the sEMG signal after the first instrumentation amplifier stage.

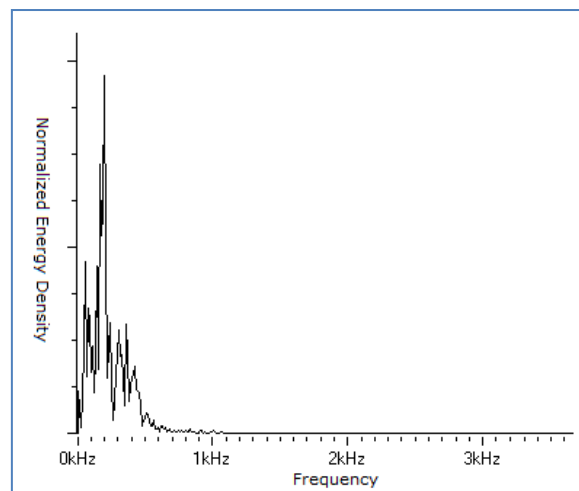


Figure 78: Measured frequency spectrum of sEMG signal

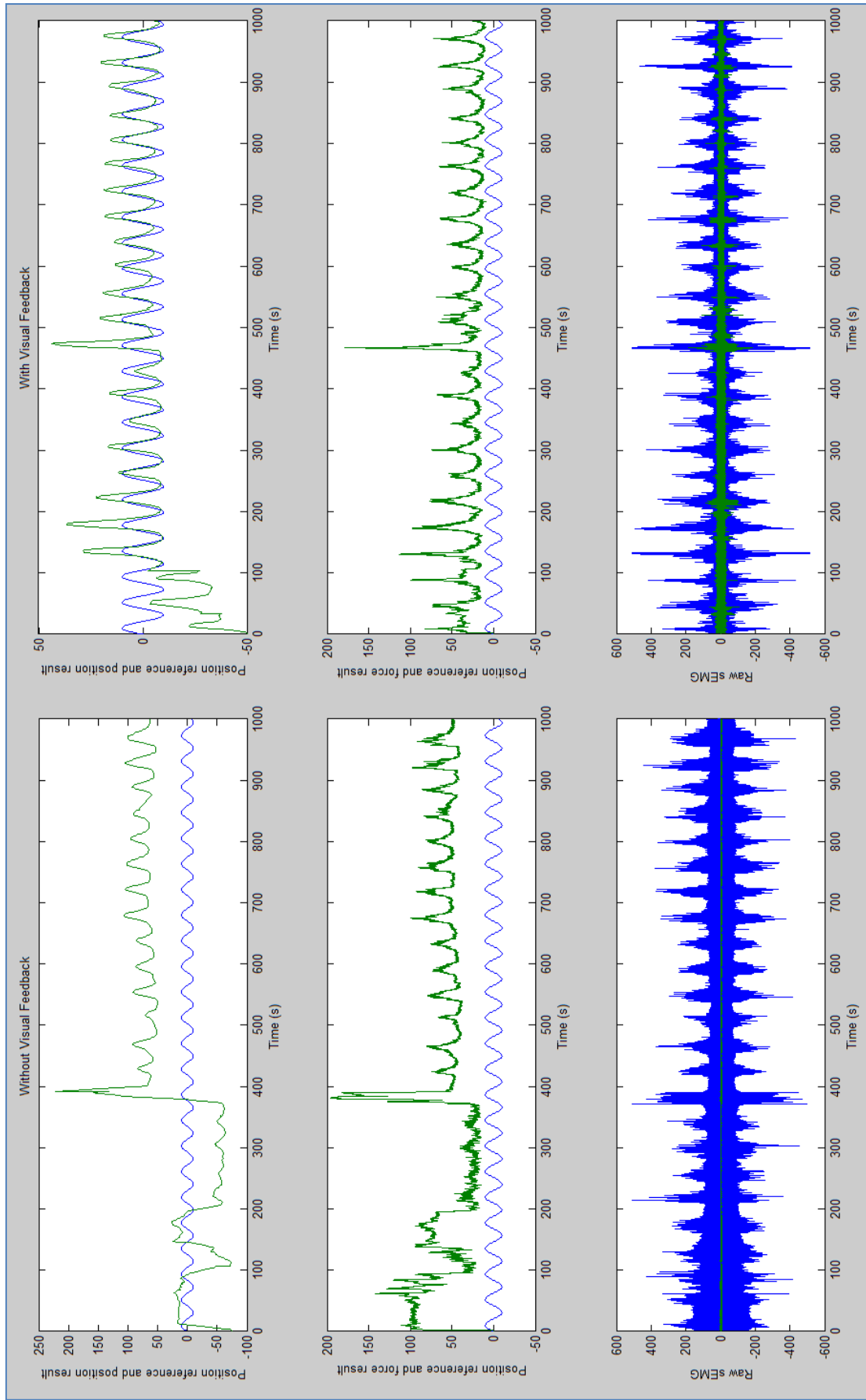


Figure 79: Worst mimic results

The passband of the 4th order band-pass filter is given in figure 80. The values are the obtained from an oscilloscope, and an input signal of 1 V p-p.

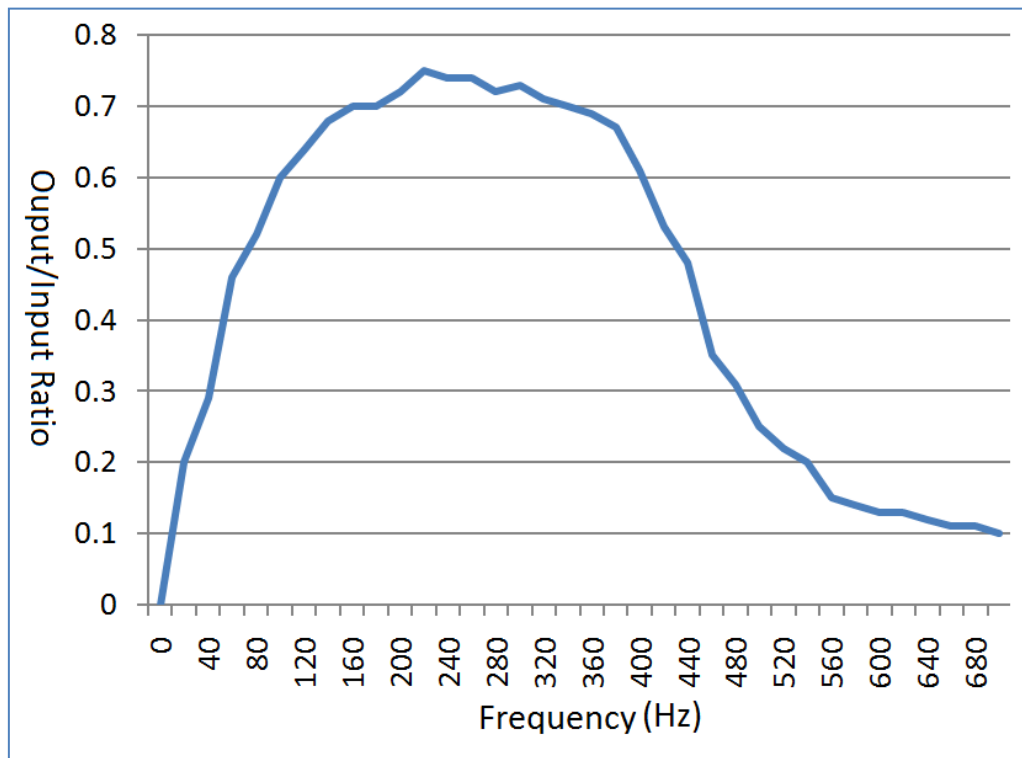


Figure 80: Pass-band of the band-pass filter

6.6.2. CALIBRATION ALGORITHM RESULTS

The noise level of the signal is compared to an ADC value of 50 during the calibration as explained in the calibration algorithm section. The prototype platform has a SNR of 10:1, but the final PCB has an improved SNR of around 50:1. The effect of the calibration algorithm is illustrated in figure 81. The graphs in the left column illustrate the sEMG platform performance before a sensor calibration. The graphs in the right column show the improved results after a sensor calibration is done.

Note in the top two plots, the range of the decoded position result (green graph) compared to the position reference (blue sine graph) improves after the sensors are calibrated. The bottom two graphs show the raw sEMG signals, with the improvement in scaling between the two antagonist muscle sEMG signal plots. The animation was not followed, therefore do not compare the reference position with the decoded position, only their amplitudes.

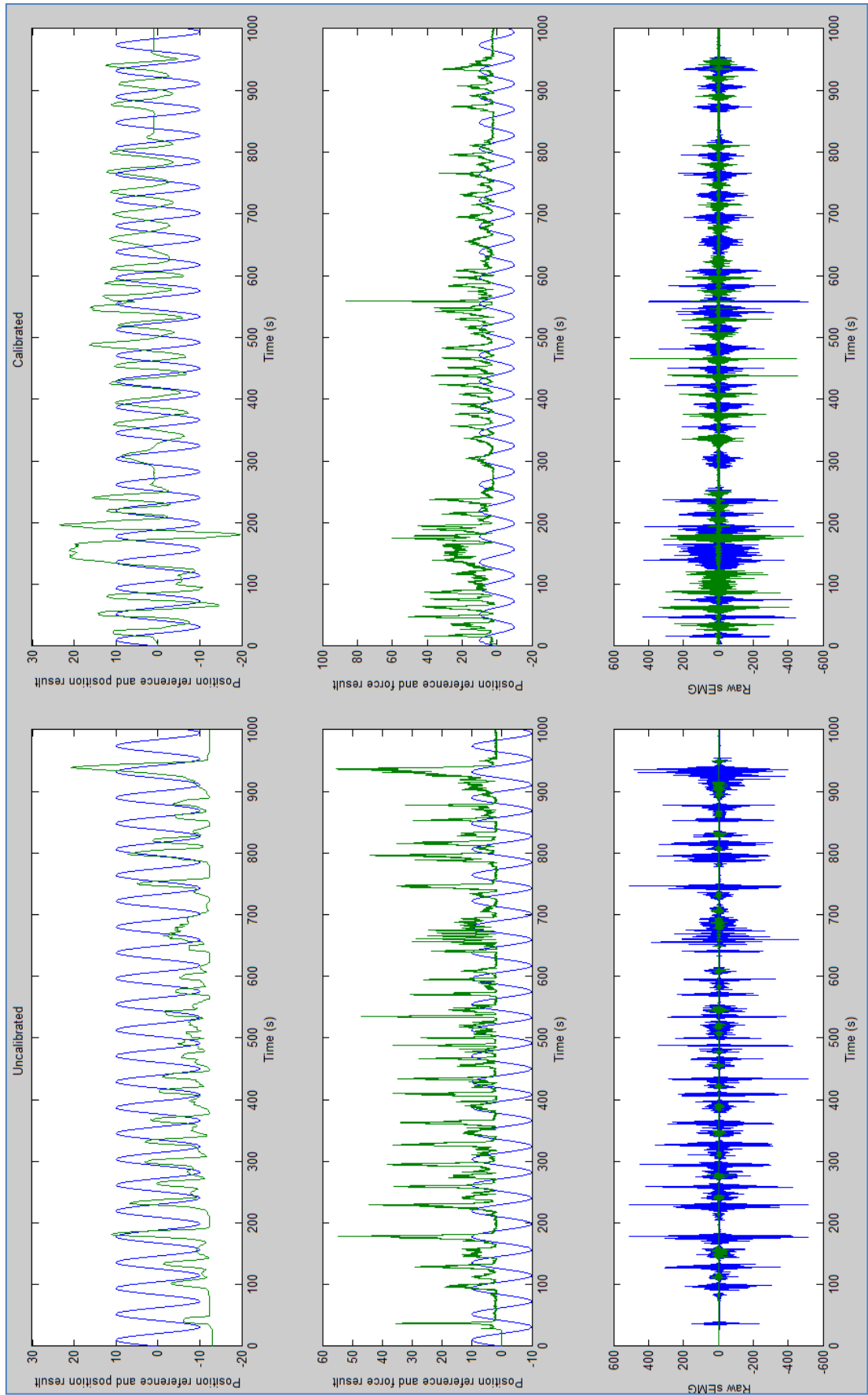


Figure 81: Calibration algorithm results

6.7. INTERESTING CASES

The sEMG platform showed positive results in the following two extreme cases.

6.7.1. THALIDOMIDE PATIENTS

A 48 year old mesomorph man who has an underdeveloped right arm was caused by Thalidomide medication. One of the greatest prescription medication disasters in medical history is the Thalidomide sleeping-pill-tranquilizer prescribed for pregnant women for morning-sickness. The medication is transferred to a developing fetus and results in abnormal limb development. He has a right forearm of about half the length of a normal person's forearm. The sEMG platform is selectively functional as he never had the opportunity to develop precise muscle movement in his underdeveloped arm. Time would be required for him to improve the precision of his muscle-movements. It is unfortunate that the sEMG simulation could not be performed on him, as he does not have a hand to compare his results to that of the normal patients.

6.7.2. TODDLERS

The sEMG sensing platform was tested on a 27 month old toddler. Although expected that the sEMG platform should sense her muscle activity, it is amazing how easily she adapted to the idea that the servo follows her hand movement. The sEMG simulation could not be performed on her either as she is not yet capable of executing the given instructions of the sEMG GUI.

6.8. CONCLUSION

The results for the simulation and test performed in the sEMG platform confirm the functionality of the complete system. The sEMG sensors frequency response ensures that the correct signals are sensed and minimal information is lost in the process. The SNR of the sensing platform is compared with the measured results of other sEMG systems. An interface with the Matlab®/Simulink® environment is demonstrated with the decoding algorithm implementation done in Simulink®. This interface is proved to be bi-directional, as Simulink® could interface with a PDM servo. The sensing platform allows Matlab®/Simulink® to provide physical output to a future prosthetic control project.

The decoding algorithm implemented in Matlab®/Simulink® demonstrates the possibility for proportional control in powered prosthesis. The testing of the sensing platform on interesting extreme cases expands the possibilities for this sEMG platform to perform further research on patients born with disabilities and cater for these patients from an early stage in their lives. The verification and validation chapter follows to compare the results to similar studies'.